
Laccolithic Emplacement of the Northern Arran Granite, Scotland, Based on Magnetic Fabric Data

C.T.E. Stevenson and C. Grove

Abstract

The Northern Arran Granite is regarded as an example of an upper-crustal granite diapir due to its sub circular outcrop and deformed aureole. However diapiric emplacement to shallow levels in the crust is physically difficult and unambiguous evidence for shouldering aside of country rocks by a diapir as opposed to shouldering due to in situ expansion of a laccolith or ballooning pluton is difficult to find. The key is in finding evidence for vertical ascent of a diapiric body where a diapir should preserve vertical stretching either around the periphery or in central portions. A laccolith on the other hand is unlikely to have consistently vertical or steep lineations but contain mainly gently plunging lineations or evidence of multiple horizontal pulses or lobes. Therefore evidence for diapiric ascent and emplacement should be dominated by vertical kinematic indicators. These structures may however be too subtle if preserved within the granite, and those in the aureole may become overprinted by late stage insitu expansion. To test whether the internal structure of the Northern Arran Granite is consistent with diapiric or laccolithic emplacement we have measured the anisotropy of magnetic susceptibility from oriented block samples from the Northern Arran Granite to determine if there are subtle or weak fabrics that will support either diapirism with vertically oriented stretching, or laccolithic emplacement where lateral emplacement is dominant and vertical motion only restricted to vertical thickening of an initially thin sheet. Our results reveal concordant dome shaped planar fabrics with mainly gently plunging or horizontal lineation, i.e. an absence of vertical stretching or flow, and

C.T.E. Stevenson (✉) · C. Grove
School of Geography Earth and Environmental
Sciences, University of Birmingham,
Birmingham B15 2TT, UK
e-mail: c.t.stevenson@bham.ac.uk

C. Grove
Department of Earth Sciences, Durham University,
South Road, Durham DH1 3LE, UK

Advs in Volcanology (2018) 377–401
DOI 10.1007/11157_2014_3
© Springer International Publishing Switzerland 2014
Published Online: 08 December 2014

possible evidence of partial lobes in the north western margins and Inner Granite. We interpret these fabrics and the deformation of the aureole in terms of dome-shaped expansion consistent with the latter model. In more detail the lineation pattern indicates convergence toward a south or south eastern point, consistent with the deepest part of the pluton (from previously published gravity modelling). Our model suggests that there may be some link to a major crustal structure (the Highland Boundary Fault) providing insight into the ascent route of the magma and possible influence of the Highland Boundary fault zone. This model also suggests that the magmatism on Arran including the central complex and sill complexes in the south of the island may have been supplied by a long lived, deeply penetrating feeder zone controlled by this major tectonic structure.

1 Introduction

The ascent and emplacement of granite as a diapiric body is a classic emplacement mechanism based on analogue models carried out by Grout (1945) using oil and corn syrup and developed by Ramberg (1967) with centrifuge experiments. However in the 1990s the ‘dykes versus diapirs’ debate (e.g. Castro 1987; Rubin 1993, 1995; Petford et al. 1993, 1994, 2000; Petford 1996a, b; Weinberg 1996; Clemens 1998; Vigneresse and Clemens 2000; Petford and Clemens 2000) casts some doubt on the diapir mechanism based largely on structural observations and numerical modelling. The principal argument for diapiric emplacement hinges on the difficulty in accounting for the amount of horizontal shortening perpendicular to the pluton margins recorded in the deformation aureole of some plutons (e.g. Paterson and Vernon 1995; Miller and Paterson 1999), i.e. the diapir model as a solution to the space problem, requires that the country rocks had flowed vertically in response to the ascent and emplacement of the diapir. The arguments against diapirs include a lack of evidence in deeply eroded terranes of the passage of diapirs (e.g. Clemens 1998; Petford and Clemens 2000), detailed examination of the kinematics of magma flow inside granite bodies that preclude upward flow but support ballooning (e.g. Holder 1980; Sanderson and Meneilly 1981; Hutton 1988; Ramsay 1989; Brun et al.

1990; Molyneux and Hutton 2000; Siegesmund and Becker 2000; Hutton and Siegesmund 2001), physical modelling of the crust which demonstrated the difficulty in ascending large batches of magma as a diapir (e.g. Petford et al. 1993) and numerical modelling which demonstrated that creation of dykes is a more efficient ascent mechanism (e.g. Rubin 1993, 1995).

The evidence for shouldering aside of country rocks due to diapiric ascent or inflation of a laccolith or ballooning pluton is ambiguous as both have been argued to produce similar features including annular or rim synforms and either radial or vertical stretching depending on the position relative to the pluton (e.g. Bateman 1985; Galadí-Enríquez et al. 2003; Paterson and Fowler 1993; Vernon and Paterson 1993). The principal parts of the diapir model are summarised in Fig. 1. In some cases the uplift of strata from beneath the pluton have been used as evidence of diapiric ascent, for example He et al. (2009) argued that strata exposed around the Fangshan pluton, Southern China, should be much deeper. The Northern Arran Granite is another example of this (England 1988, 1990, 1992) (Fig. 2).

The principal tenet of the diapir model is vertical movement of the entire body as opposed to situ expansion with or without doming from an initially laterally emplaced tabular or sill-like body as in a laccolithic/ballooning style emplacement (cf. Fig. 1). Therefore the current study aims to test the diapir emplacement model

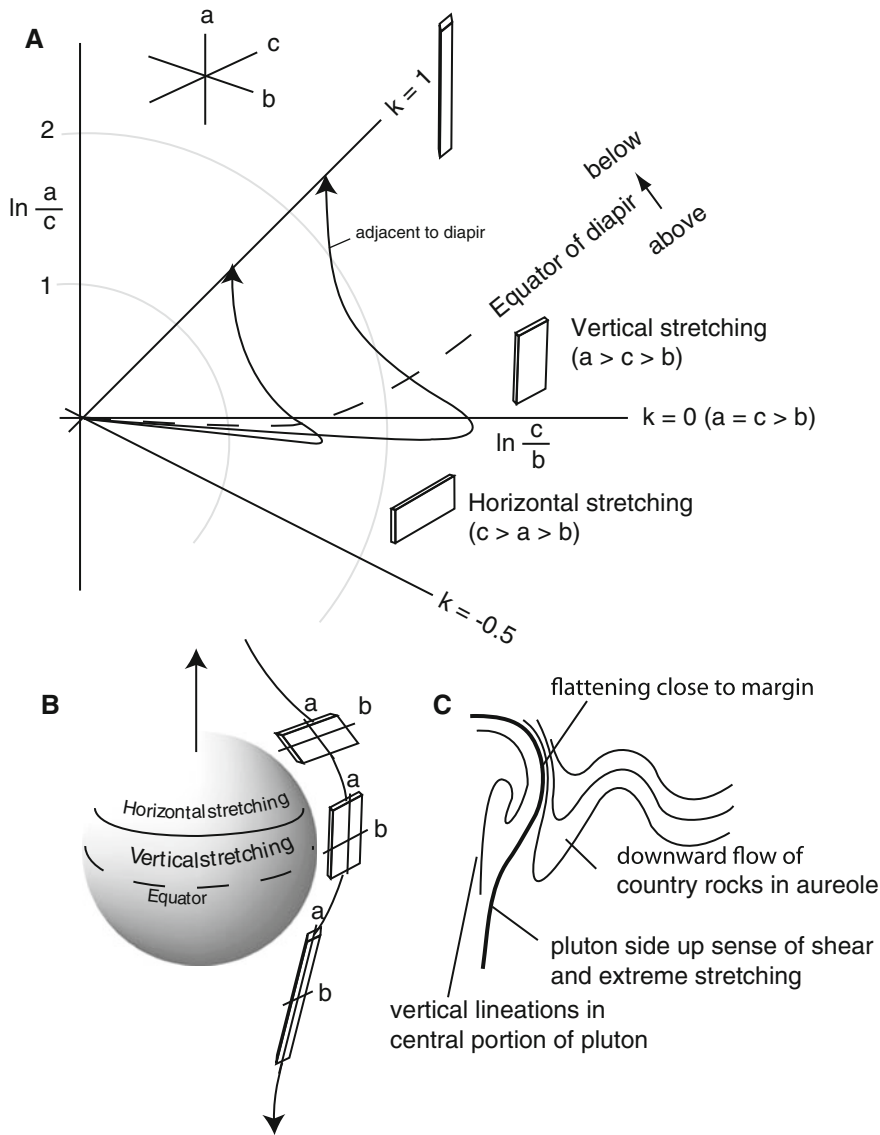


Fig. 1 **A** Model for the evolution of strain in the aureole of a rising diapir after Cruden (1988). This diagram illustrates how vertical stretching should be observed above the equator of the diapir. The principal axes a , b and c are Cartesian where b and c are horizontal and a is vertical. These are also relative to the diapir where b is radial and c is tangential; a becomes deflected as the

diapir passes. **B** Illustrates diagrammatically the evolution of strain using the system described in part A, emphasizing the relative disposition of vertical stretching, i.e. when a becomes the longest axis. **C** typical model for the fabrics in and around a rising diapiric body drawn as a semi-cross section (cf. Cruden 1988)

by examining deformation of the granite itself by attempting to identify evidence for vertical ascent. Anisotropy of magnetic susceptibility (AMS) measurements have proven to be a sensitive fabric analysis tool especially when applied

to granitic rocks (e.g. Bouchez 1997; Borradaile and Henry 1997; Borradaile and Jackson 2004) and would be able to detect any subtle evidence of vertical movement (such as vertical stretching) as long as it has not been completely obliterated

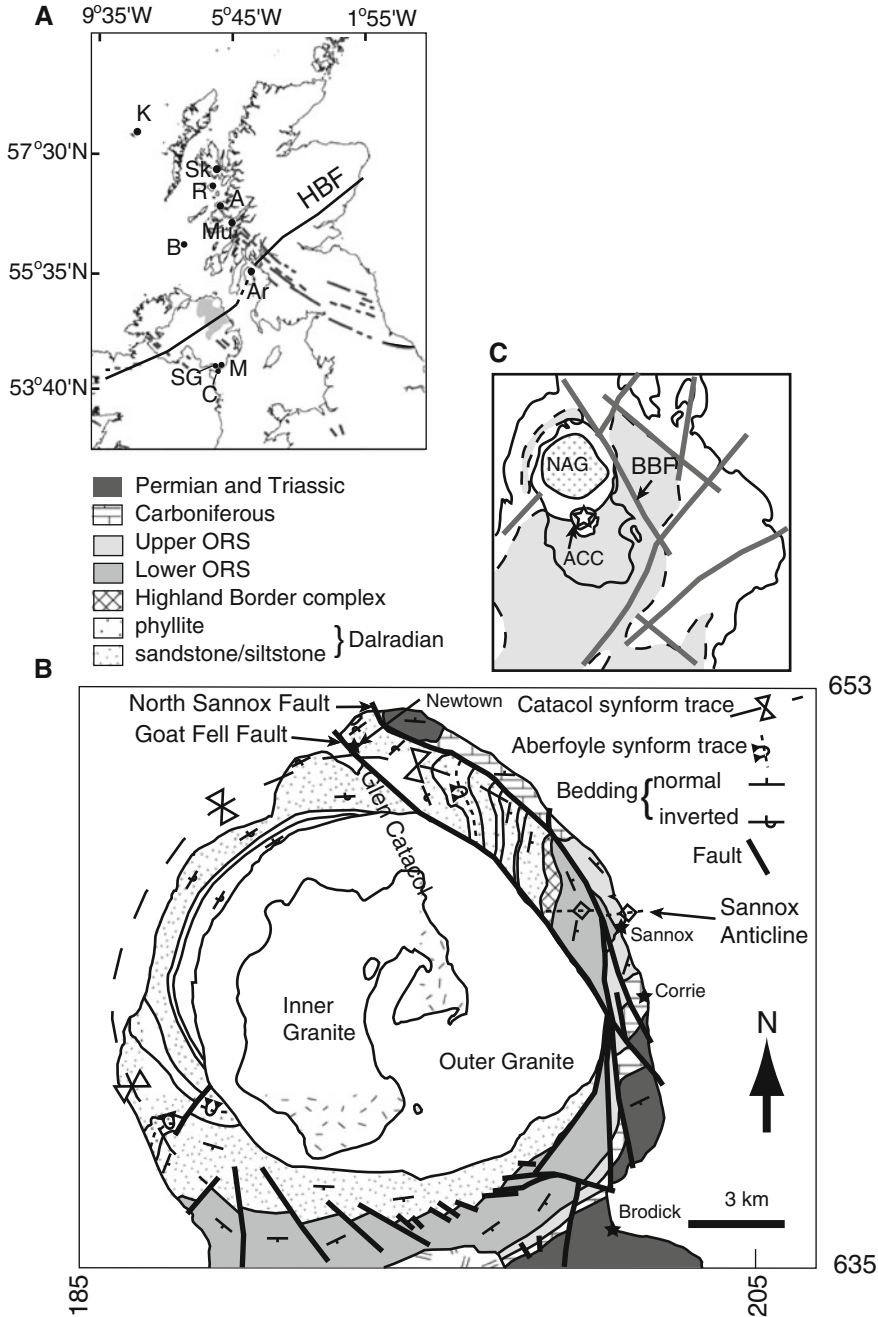


Fig. 2 A Location of the main igneous centres in the British and Irish Palaeogene Province: *S&C* Slieve Gullion and Carlingford, *M* Mournes, *Ar* Arran granite, *Mu* Mull, *A* Ardnamurchan, *R* Rhum, *Sk* Skye, *K* St. Kilda (adapted from Bell and Emeleus 2004; Cooper and Johnson 2004). **B** Simplified geological map of the north of Arran. Location indicated by British National Grid

numbers from square NR. Redrawn from Woodcock and Underhill (1987); Hull et al. (1987). *ORS* Old Red Sandstone. **C** Distribution of off shore faults around the Isle of Arran. Grey area indicates extent of outcrop of New Red Sandstone (NRS) enclosed by a dashed line when off shore and a solid line onshore. *BBF* Brodick Bay Fault. Redrawn from Woodcock and Underhill (1987)

or totally overprinted by late stage expansion or tectonic deformation.

Our magnetic fabric results indicate that there is expansion, consistent with the deformation in the aureole during in situ expansion. There are however no consistently vertical or steeply plunging linear fabrics but a tendency toward gently plunging concentric stretching which supports lateral emplacement followed by domed expansion in situ. In central and north western portions, foliations are usually gently dipping and any linear components are also gently plunging. The fabric pattern allows us to reconstruct the unroofed portion of granite, which takes the form of a dome up to 5 km thick at its culmination (i.e. ca. 3.5–4 km unroofed granite). We argue that in the case of an expanded diapir, that if radial stretching was extreme to the point of obliterating or overprinting vertical linear fabrics, then it should be recorded pervasively and fabrics in the Inner Granite should be continuous with fabrics in the Outer granite. What is preserved however only shows occasional steeply plunging lineations and a variable fabric. We conclude that this fabric is more likely to be modified fabrics of an expanded incrementally assembled tabular pluton, similar to a laccolith (*sensu* Cruden 1988), rather than a diapir. We suggest that the host rock deformation may be explained by shouldering during doming and not necessarily by diapiric uplift. We then examine the implications for the evolution of the Highland Boundary Fault zone in light of our emplacement model and links to other igneous centres on Arran.

2 Geological Background

The oldest rocks that crop out around the Northern Arran Granite are meta-sediments of the mid-Neoproterozoic to early Ordovician Dalradian Supergroup (Fig. 2B). The Dalradian Supergroup comprises mainly clastic meta-sediments with some volcanic units that were deposited from around 730 Ma, during the break-up Rhodinia, onto the continental slope of what would become Laurentia (Stephenson et al. 2013) and underpins much of the geology of NW

Scotland and Ireland. The Dalradian rocks on Arran consist of greenschist facies interbedded meta-pelites and meta-psammites with beds between 0.5 and 1 m thick (England 1988) and have been correlated to the Southern Highlands Group (Harris et al. 1978; Halliday et al. 1989; Tanner 2008). The Dalradian rocks crop out to the north, west and south of the Northern Arran Granite today.

The Dalradian strata were deformed during Caledonian polyphase deformation (480–500 Ma), resulting in the NE–SW trending downward facing Aberfoyle anticline (Shackleton 1957; England 1988). The Dalradian meta-sediments are faulted against the younger rocks by the Highland Boundary Fault (HBF) which has an uncertain trace in northern Arran (Woodcock and Underhill 1987; England 1988; Tanner 2008) (Fig. 2A).

The HBF is a major terrane boundary that separates the Grampian Terrane to the north–west, which is dominated by Dalradian meta-sediments and Caledonian aged plutons, from the Mildand Valley Terrane to the south–east, which is dominated by late-Silurian to early-Carboniferous sediments and volcanics (Tanner 2008). The HBF is currently manifest at the surface as a mid-Devonian steep reverse fault, although it may have begun as a transcurrent fault as early as 420 Ma (see Tanner 2008 for detailed discussion).

The Ordovician age Highland Border Complex (HBC) lies just beneath the younger Devonian rocks and marks the end of the Caledonian sequence on Arran (Fig. 2B). This complex was obducted onto the Grampian Terrane and consists (on Arran) of black shale and spilite (England 1988), it crops out along the accepted trace of the HBF in the north of the island, and is cut by the granite. The Devonian sediments of the ‘old red sandstone’ are faulted against the Dalradian rocks in the north of the island and overlie Dalradian sediments to the south of the northern Arran Granite.

The post-Devonian rocks were deposited in a rift basin, with evidence of syn-sedimentary faulting and consist of Carboniferous limestones conformably overlain by Permian fluvial mudstones, siltstones and sandstones which crop out to the east of the granite. The rocks within the

Midland Valley Terrane are commonly faulted, the system of NNW–SSE trending faults east of the granite including the Goat Fell Fault and the North Sannox Fault (probably also including the off shore Brodic Bay Fault) is called the Laggan Fault Zone (Woodcock and Underhill 1987) (Fig. 2B, C). This system downthrows to the east and was active during deposition Palaeozoic sediments and were reactivated in the Palaeogene during the emplacement of the granite (McLean and Deegan 1978; Woodcock and Underhill 1987; England 1988).

3 The British and Irish Palaeogene Igneous Province

The British and Irish Palaeogene Igneous Province (BIPIP) here refers to all the onshore igneous material that was extruded and emplaced mainly in north–west Britain and Ireland during the early to mid-Palaeogene (ca. 55 Ma) (Fig. 3). Some studies refer to the North Atlantic Igneous Province which includes all the igneous activity in north–west Britain and Ireland, Faroe Islands, Iceland and East Greenland, including all off-shore occurrences (e.g. Jolley and Bell 2002; Jolley and Widdowson 2005; Meyer et al. 2007). Other studies are more restricted to the intrusions and volcanics of north–west Scotland and refer to the British Palaeogene Igneous Province (BPIP) (e.g. Brown et al. 2009). Older work refers to Tertiary (now Cenozoic) instead of Palaeogene (e.g. Emeleus et al. 1992).

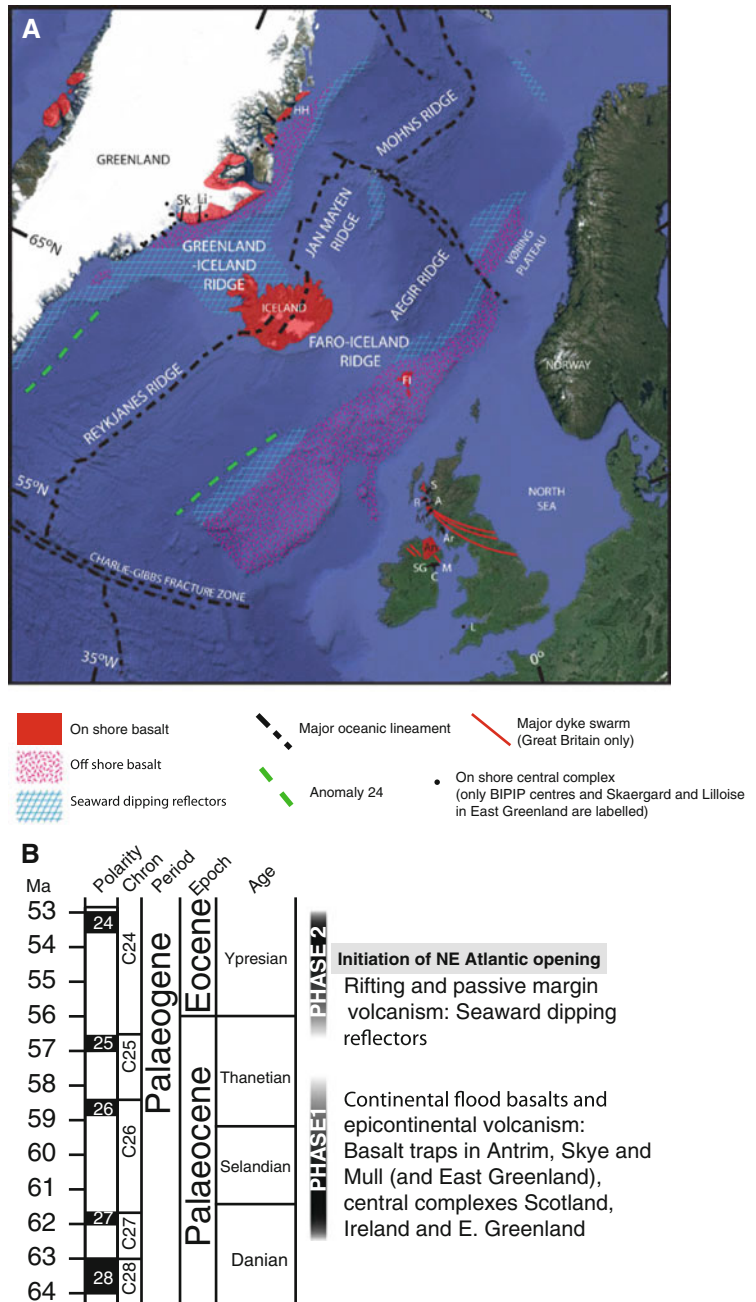
The BIPIP is a classic region for volcanologists and produced several of the key models for upper-crustal igneous emplacement that guide our current understanding of volcanology. The BIPIP is famous for exposing geological features that document extrusive activity as well as deeply eroded volcanic edifices and the subsurface volcanic plumbing. There are a number of extremely useful general reviews of the BIPIP (and NAIP) (Thompson 1982; Emeleus et al. 1992; Saunders et al. 1997; Trewin 2002) and guides (e.g. Emeleus and Bell 2005) available for

more detailed information and in-depth discussion on these features. In this contribution we will highlight some of the most important features which are found in NW Scotland, Inner Hebrides and Northern Ireland (Figs. 2A and 3) and include basalt traps in Antrim, Mull, Skye, Rum, Muck and Eigg; dolerite sill complexes in Skye and Antrim, central complexes found on Mull, Skye, Ardnamurchan, Rum, Arran, Slieve Gullion and Carlingford; and anorogenic granite plutons including the Mourne Granite Centres, Western Red Hills of Skye, Northern Arran Granite, the Ailsa Craig and the Lundy granite.

3.1 Plume Related Origins

The magmatism that generated the BIPIP intrusions and volcanics is now widely accepted to be linked with impingement of the proto-Icelandic plume into the base of the Laurasian crust in the early Palaeocene and subsequent break-up of this continent into Laurentia (N. America and Greenland) and Eurasia (Europe and Asia) around 56 Ma (Doré et al. 1999; Jolley and Bell 2002; Trewin 2002; Meyer et al. 2007; Saunders et al. 2007). The initial effects of the plume event were marked by a rapid and short-lived uplift of Mesozoic basins in this region at the Cretaceous–Palaeogene boundary 65 Ma followed roughly 2–3 Myr later by more uplift and the earliest onset of volcanism (Phase 1 of Saunders et al. 1997; see also Trewin 2002). Phase 1 continued for roughly 4 Myr and included the main phase of continental flood basal eruption resulting in basal-t traps in Antrim, Skye and Mull (as well as East Greenland). During this time most of the on-shore BIPIP activity took place (Saunders et al. 1997). The second major phase of activity began around 56 Ma and heralded the opening of the North Atlantic at 55–54 Ma. This phase included passive margin volcanism and has resulted in a series of seaward-dipping reflectors in the North Atlantic and off-shore East Greenland (Saunders et al. 1997). The timing of phases 1 and 2 magmatism in the NAIP is summarised in Fig. 3.

Fig. 3 **A** Map showing the main features of the NAIP (see text for explanation) (taken from Saunders et al. 1997; Trewin 2002; Emeleus and Bell 2005). **B** Summary chart of the main phases of activity that formed the NAIP with special reference to the BIPIP (from dates reported in Saunders et al. 1997; Emeleus and Bell 2005). In this chart the date in millions of years before present (Ma), polarity (magnetic polarity), chron (magnetostron), period, epoch and age are all taken from the current USGS chronostratigraphic chart



3.2 Magma Genesis and Evolution

The magma that formed the BIPIP was generated by fractional crystallisation of melt derived from depressurized upper mantle (Saunders et al. 1997;

Ellam and Stuart 2000). This was triggered by the thermal uplift caused by the proto-Icelandic plume. The 1st phase of magmatism was varied but dominated by basalts. These were of transitional alkali and tholeiitic varieties reflecting the

respectively lower and higher structural level at which their parent melts were generated (Saunders et al. 1997).

The great variety of magma types in the BIPIP (and the initial phase of the NAIP) is most likely due to contamination of basaltic magma from the continental crust through which it ascended. Many studies have focused on identifying sources for magma contamination focusing on two isotopically distinct lower crustal sources; viz. granulite and amphibolite, based mainly on the lower $^{87}\text{Sr}/^{86}\text{Sr}$ of the granulite gneiss (Saunders et al. 1997). Various other mid and upper crustal sources have also been included in similar contamination studies of BIPIP magmas (e.g. Thompson et al. 1986; Wallace et al. 1994; Troll et al. 2005; Meyer et al. 2009; Meade et al. 2009).

3.3 Central Complexes

Central complexes, or centres, mostly formed during phase 1 of the NAIP magmatism. These features are the most relevant aspect of the BIPIP to this volume as they preserve a range of exposure levels of large and explosive volcanic edifices, from surface calderas (e.g. Central Arran) to deeply eroded sill, dykes and magma chambers (e.g. Ardnamurchan) and are where some of the classic models for ring-dyke and cone-sheet systems were developed (Bailey 1924; Richey 1928, 1932; Richey and Thomas 1932; Anderson 1937). A central complex in the BIPIP usually consists of a sub circular outcrop of igneous rock greater than c. 5 km diameter with steeply dipping external boundaries. Central complexes are often highly heterogeneous including crescent shaped or annularly distributed internal variations. The internal structure of these is often taken to be subvertical or steeply outward dipping following the ring-dyke model of Richey (1928). It is in the component parts of central complexes where early workers developed some of the key models that guide our current understanding of volcanology. The specific emplacement models that were developed to their current understanding in the BIPIP are cauldron subsidence (Bailey 1924),

ring-dyke (Richey 1928) and cone-sheet (Anderson 1937).

Ring-dykes: A ring-dyke is an annular or crescent shaped intrusion with steep boundaries outwardly dipping about a central point. The model involves the downward movement of a central block, such that they represent essentially magma filled reverse faults. The intrusive material in a ring-dyke emanated from an underlying magma chamber into which the central block foundered. Ring-dykes are linked to caldera volcanoes, where they then provide vent structures, and cauldron subsidence (described next).

Cauldron subsidence: This is essentially the subterranean version of a caldera volcano where, instead of erupting, the ring-dyke stops propagating upwards and propagates toward the centre to form a roof. The relationship with a subjacent magma chamber is the same as a caldera volcano.

Cone-sheet: These form confocally dipping sheets. They could be regarded as the opposite of ring-dykes to the extent where a ring-dyke is formed when buoyancy permits a large block to founder, cone-sheets are formed due to excess magma pressure in a magma chamber, greater than buoyancy, that forces up the roof. Cone-sheets are the resultant magma-filled fractures.

The elegant way that these models link together to explain the dynamics of upper-crustal magma emplacement often requires, however, a superficial treatment of the space problem (assuming assimilation is volumetrically insignificant, the volume of country rocks now occupied by intrusive igneous material must be accounted for). It is worth considering this issue and putting the current study in the context of recent work on the emplacement of key centres in the BIPIP.

3.4 Recent Work on the Emplacement of Some Centres

The plate tectonics paradigm and 20th century advances in geophysical techniques have come along since the early work in the BIPIP generated

these classic models. Walker (1975) attempted to draw together geophysical evidence of positive gravity anomalies often observed beneath central complexes and the association of mafic and felsic magmas in a unified generic model that could explain most features of typical BIIP centres. This model was the first to attempt to explain the BIIP on a crustal scale and involved a diapir that ascended to a high level in the crust. This diapir caused doming at the surface resulting in a caldera edifice including ring dykes and surrounded by cone-sheets. The diapir was followed by denser mafic magma that was emplaced at the base of the main granitic body and caused isostatic equilibrium of this buoyant body. As isostatic equilibrium was reached, subsidence occurred resulting in the formation of cauldron subsidence.

A number of recent studies have offered some alternative emplacement models for each of these key examples using novel data on the internal fabrics and structure of the intrusions using anisotropy of magnetic susceptibility analyses (e.g. O'Driscoll et al. 2006; Stevenson et al. 2007a, 2008; Petronis et al. 2009; Stevenson and Bennett 2011; Magee et al. 2012a, b). O'Driscoll et al. (2006) showed that the Ardnamurchan Great Eucrite is more likely a lopolith with an inverted cone shaped geometry than a traditional ring-dyke. Stevenson et al. (2007b) and Stevenson and Bennett (2011) revealed internal fabrics in the Mourne Granite centres (Eastern and Western respectively) that supported a laccolithic as opposed to cauldron subsidence emplacement, principally from the dome shaped foliation disposition and lateral lineation direction. Other evidence in this study included deformation of the host rocks and previously published geophysical data. Stevenson et al. (2008) studied the Slieve Gullion Ring Complex, focusing on the granitic ring-dyke part. This study concluded that the traditional ring-dyke model was not unambiguously supported and presented an alternative interpretation that included laterally emplaced sheets cut by ring-faults. In addition to Stevenson et al. (2008), Emeleus et al. (2012) have highlighted and reiterated Richey's (1928) observations regarding Slieve Gullion, presenting a

strong argument in favour of a traditional ring-dyke model emphasising the relationships between fault rocks and tuffsites. Magee et al. (2012a) used AMS data to test the classic cone sheet emplacement model for the archetypal Ardnamurchan cone-sheet swarm. The data revealed dominantly lateral magma flow directed around the Ardnamurchan centre rather than emanating from beneath it. This observation coupled with some simple mechanical modelling produced a model that described magma exploiting concentric fractures and not necessarily creating them. The implication was that the cone-sheet magma may have emanated from the nearby Mull igneous centre and therefore intrusions from nearby centres can overlap. This conclusion was supported by Magee et al. (2012b) who, in a related study, found the Ben Hiant dolerite intrusion on Ardnamurchan was emplaced in a northwestward direction toward the Ardnamurchan centre and from Mull and not the other way round.

4 The Northern Arran Granite

The Northern Arran Granite is roughly sub-circular in outcrop with a maximum diameter of 13 km (Fig. 2B). The granite consists of two distinct units: an inner fine-grained granite which intruded an outer coarse-grained granite (Bell and Williamson 2002; Emeleus and Bell 2005). In general the granite is mineralogically homogeneous. Any variations are subtle and it can be described as a medium to coarse-grained weakly porphyritic biotite syenogranite. The Northern Arran Granite was intruded into the country rocks described above at between 60.5 and 58.5 Ma from Rb-Sr and $^{40}\text{Ar}/^{39}\text{Ar}$ dating respectively (Dickin and Bowes 1991; Dickin 1994; Mussett et al. 1988) at around 4–5 km depth (Woodcock and Underhill 1987).

The country rocks surrounding the granites are thermally affected within 500 m of the granite with a maximum temperature of 550 °C in contact with the granite, no muscovite is present in the metamorphic aureole (England 1988). In the west the granite is in contact with Dalradian

rocks where the contact is characterised by a region of sheared contact metamorphosed rock. The eastern contact is marked by the Goat Fell Fault which is downthrown to the east, the fault brecciates the granite on a microscopic scale (England 1988).

The Northern Arran Granite was produced by contamination of basic differentiates by crust resembling exposed Dalradian units (Dickin 1994) associated with a mantle plume (Meighan et al. 1992). Both granites contain drusy cavities which are interpreted to occur in sheets (England 1988) but cannot be traced over distance due to poor outcrop quality. The cavities are frequently lined with quartz, alkali feldspar and mica together with several rare minerals (Emeleus and Bell 2005). The most recent and comprehensive petrological assessment was carried out by England (1988) who identified three petrographical zones within the coarse-grained granite and six drusy layer bound sheets within the fine-grained granite.

4.1 Previous Work on the Emplacement of the Northern Arran Granite

The Palaeogene aged Northern Arran Granite (Fig. 2) has been interpreted as an upper crustal diapiric intrusion by England (1988). This pluton has a roughly circular outcrop with an approximately 11 km diameter and is situated close to where the Highland Boundary Fault should cross the island (Anderson 1947; Stone and Kimbell 1995; Pharaoh et al. 1996; Emeleus and Bell 2005; Tanner 2008; Woodcock and Strachan 2012). The Northern Arran Granite comprises two units; a relatively fine grained Inner Granite and a relatively coarser grained Outer Granite. It was emplaced into Dalradian interbedded sandstone and phyllite, and Devonian Old Red Sandstone at 60.3 ± 1.6 Ma (Dickin et al. 1981).

The diapiric emplacement model for the Northern Arran Granite is based mainly on the deformation of the aureole in particular the formation of a rim synform, the Catacol Synform,

which refolds a downward facing Caledonian fold, the Aberfoyle Synform (England 1988, 1990, 1992). The key part of this model is that the formation of the Catacol Synform to its current geometry involved the uplift of one limb of the Aberfoyle Synform by 2–3 km and thus required the ascent of the granite body over a distance greater than its radius precluding an expansion (ballooning) model. England (1992) explained that the dominant flattening strain was due to late stage radial expansion of the granite that overprinted the early vertical stretching. The lack of steep lineation, England (1992) argued, was consistent with the predicted pattern of deformation around a rising diapir recorded above the equator according to Cruden (1988).

Gouly et al. (2001) presented a gravity model for the Northern Arran Granite that yielded a horizontal floor 0.3–1.2 km deep, much shallower than expected from a roughly spherical diapir. The shape of the pluton according to Gouly et al. (2001) was a laccolith although Gouly et al. (2001) concluded that there may have been significant lateral or radial expansion—‘mushrooming’—to achieve this shape and ultimately did not dispute the diapir model.

However, aside from the physical difficulties in ascending a mass of molten magma of required proportions to a high level in the crust (e.g. Petford et al. 2000), the evidence for upward motion of the diapir either from inside the granite or in the aureole, including vertical stretching in the aureole or near the margins in the granite or in any central portion of the granite (Schmelling et al. 1988; Cruden 1988, 1990) (Fig. 1) are lacking. This problem is compounded by the possibility that a diapir may expand in situ as further diapiric pulses enter the pluton from beneath or if the diapir flattens or mushrooms at a late stage. The key of this model therefore is, given the roughly equatorial (or just above the equator) position of the current exposure level (based on England 1988), vertical stretching should be present in central portions even if it has been modified or obliterated at the margins. We would also expect evidence of ‘pluton up’ sense of shear.

5 Anisotropy of Magnetic Susceptibility Analyses

Anisotropy of magnetic susceptibility (AMS) is a measure of the variation of the magnetic susceptibility with orientation of a sample. In rocks the AMS signal is usually controlled by the orientation and distribution of magnetite grains and sometimes biotite, pyroxene or other Fe bearing minerals (Tarling and Hrouda 1993). Because magnetite is often aligned with, forms inclusions within or forms around the main rock forming silicate phases, AMS data usually provides information about the preferred orientation of silicate minerals and has often been used as a fabric analysis technique (e.g. O'Driscoll et al. 2008). AMS is particularly useful when visible fabrics are too weak or subtle to be recorded otherwise.

Thirty-eight oriented samples were collected from mainly the northern and eastern portions (most accessible and best exposed) of the Northern Arran Granite. From these samples an average of 10 sub specimens were taken (each 10 cm³), according to the methods outlined by Owens (1994). The AMS of each sub-specimen was measured at the University of Birmingham using an Agico KLY-3S Kappabridge. Data from each sub-specimen were subject to statistical analysis according to Jelinek (1981). Both the statistical analysis and reorientation of data from the specimen frame to the geographical frame were carried out using a modified version of Anisoft (supplied by M. Chadima, personal communication 2013). Data calculated for each station using Jelinek (1981) statistics which assumes that the data represents a single multi-normal population.

The AMS signal may be viewed as a second order ellipsoid in which three orthogonal principal susceptibilities are defined. The AMS signal thus has 6 linked quantities; the orientation of each principal susceptibility axis and their magnitude. In this case we use volumetric susceptibility, K , which is equal to the applied field divided by the resultant magnetisation. The kappabridge that we used measures the difference

in the field detected by a pickup coil caused by the presence of a sample. As the sample is rotated inside this coil, the change in field is detected and produces a sine curve. This is repeated in three orthogonal reference positions and a final control reading taken along a single axis (bulk susceptibility of K_{bulk}) is used to calculate the complete tensor.

In this contribution we will use conventional parameters to report AMS data. The components of the AMS tensor are as follows: Maximum susceptibility axis is K_1 , intermediate susceptibility axis is K_2 , minimum susceptibility axis is K_3 , mean susceptibility (taken as the susceptibility representative of a particular station) is equal to $(K_1 + K_2 + K_3)/3$. There are then a series of linked parameters that describe the shape and anisotropy of the tensor. These are the lineation strength, L , which is equal to K_1/K_2 , the foliation strength, F , which is equal to K_2/K_3 . The total anisotropy, P' (a more sophisticated version of $P = K_1/K_3$ which includes K_2) is defined by (after Jelinek 1981):

$$\ln P' = \sqrt{2((\eta_1 - \eta_m)^2 + (\eta_2 - \eta_m)^2 + (\eta_3 - \eta_m)^2)^{1/2}}$$

In the case of L , F and P' , the values start at a minimum of 1 and may be roughly converted to percentage as 1.01 = 1 %, 1.05 = 5 %, 1.10 = 10 % and so on. The shape parameter, T , is calculated as follows:

$$T = (2\eta_2 - \eta_1 - \eta_3)/(\eta_1 - \eta_3)$$

where $T = -1$ is prolate, $T = 1$ is oblate and $T = 0$ is triaxial. It is standard practice to plot T against P' , however we note here that this style of plot is of limited use at very low anisotropies as the uncertainty of the shape at very low anisotropies is not accounted for in the T value because as P' tends to 1.0 the errors of T tend to infinity (Tarling and Hrouda 1993).

In addition to the definition of these parameters, the AMS data is also plotted stereographically on lower hemisphere equal area plots. The orientation of the three principal susceptibilities are plotted along with 95 % confidence limits.

To test the effect of outlying data we have stripped anomalous data from each station (original data is also reported) and assessed the effect on the overall fabric orientation. No obvious examples of sub-populations which seem to represent more than one fabric orientation within a station are seen. The rules applied to the data rejection are: (1) all 3 axes must be $>40^\circ$ outside 95 % confidence ellipses; (2) when only 2 axes are anomalous (and not obviously due to inverse fabric) then the mean shape parameter was considered such that a dominantly linear AMS signal K_1 axes significantly outside confidence ellipses are more likely to be anomalous. It is impossible for only one axis to be anomalous. Where samples had weak signals then data selection was avoided. This exercise never significantly altered fabric orientations (generally $<10^\circ$ or within original confidence ellipse).

6 AMS Results

The AMS data for the Arran Granite is summarised in Table 1 and plotted graphically in Fig. 4. K_{mean} is between 1.98×10^{-4} and 3.47×10^{-2} similar other Palaeogene granitoids in Britain and Ireland (Table 2) and consistent with a magnetite concentration of 0.001–0.1 wt% (Tarling and Hrouda 1993). P' ranges between 1.049 and 1.007. T values are scattered but tend marginally toward oblateness.

6.1 Magnetic Fabrics

The AMS tensor may be simplified to derive structural data in the form of a plane (normal to K_3) and a lineation (parallel to K_1) where the shape and confidence ellipses permit. This data is plotted on Fig. 5 which allows an overview of the fabric pattern. Figure 4 highlights that there is no obvious relationship between P' and T, but a positive trend (tendency to oblateness with higher P') is discernible. This allows us to plot a summary of the fabric in Fig. 6. Overall the AMS data describe a concentric and dome-like foliation in

the east and south east, with a dominantly sub-horizontal and north–south trending lineation (Figs. 5 and 6). In this region the foliation is slightly stronger (Figs. 5 and 6).

To the northwest, the fabric is weaker and more irregular but in general can be described by a dominantly sub horizontal foliation and lineation except close to the granite boundary where the foliation tends to be steep and concentric. In addition there is a zone along Glen Catacol (Fig. 6) where fabrics seem discordant to any overall trend. Here they are steep and trend north–south.

7 Insights into the Structure of the Northern Arran Granite and Surrounding Deformation Aureole

7.1 Geometry of Granite Contacts

The boundary of the Outer Granite is mainly steeply dipping or near vertical. The Inner Granite however seems generally to have gently dipping contacts across the central portions of its outcrop. England (1988) suggested that the Inner Granite was emplaced due to foundering of a large block of Outer Granite in a cauldron subsidence style model. In this model a vertical fracture near the north west of the Outer Granite somehow ceased to propagate upward and instead propagated laterally to the south east causing a large block of Outer Granite to founder into a magma chamber of Inner Granite magma.

8 3D Geometry of the Pluton

The overall pattern is of a dome shaped foliation with a generally subhorizontal lineation. No consistent vertical lineation pattern is found and lineations near the margins are usually gently plunging. This appears to be more consistent with a laccolithic model. The unusual fabric pattern found in Glen Catacol may represent some kind of late magmatic shear zone where partially

Table 1 AMS data

| Sample | 1,000 km grid system | | K_{mean} ($E^\circ - 3$) | L | F | T | P' | Pole to foliation (K_3) | | | Foliation plane | | | Lineation (K_1) | |
|--------|----------------------|----------|-------------------------------------|------|------|-------|------|-----------------------------|--------|-----|-----------------|--------|---------|---------------------|--|
| | Easting | Northing | | | | | | Azimuth | Plunge | Dip | Dip azimuth | Plunge | Azimuth | | |
| AG 1 | 191650 | 645532 | 3.25 | 1.00 | 1.30 | 0.97 | 1.04 | 120 | 82 | 8 | 300 | 294 | 8 | | |
| AG 2 | 191760 | 645873 | 3.50 | 1.01 | 1.01 | 0.34 | 1.02 | 340 | 1 | 89 | 160 | 70 | 33 | | |
| AG 3a | 191877 | 646066 | 3.95 | 1.01 | 1.03 | 0.54 | 1.04 | 114 | 77 | 13 | 294 | 167 | 2 | | |
| AG 3b | 191879 | 646070 | 1.68 | 1.01 | 1.02 | 0.38 | 1.02 | 123 | 63 | 27 | 303 | 344 | 21 | | |
| AG 4 | 191984 | 646304 | 3.80 | 1.01 | 1.02 | 0.36 | 1.03 | 94 | 71 | 19 | 274 | 186 | 1 | | |
| AG 5 | 192142 | 647971 | 4.32 | 1.01 | 1.00 | -0.49 | 1.01 | 331 | 54 | 36 | 151 | 62 | 1 | | |
| AG 6 | 192100 | 648138 | 4.75 | 1.01 | 1.02 | 0.26 | 1.02 | 157 | 11 | 79 | 337 | 20 | 75 | | |
| AG 7 | 192021 | 648302 | 4.47 | 1.02 | 1.02 | 0.09 | 1.03 | 182 | 42 | 48 | 2 | 357 | 48 | | |
| AG 10 | 195186 | 646483 | 1.06 | 1.00 | 1.00 | 0.03 | 1.01 | 25 | 55 | 35 | 205 | 256 | 24 | | |
| AG 11 | 195213 | 646648 | 1.16 | 1.01 | 1.01 | 0.35 | 1.02 | 101 | 20 | 70 | 281 | 196 | 11 | | |
| AG 14 | 195142 | 647546 | 1.87 | 1.01 | 1.03 | 0.34 | 1.04 | 262 | 2 | 88 | 82 | 162 | 76 | | |
| AG 16 | 195055 | 647965 | 2.26 | 1.01 | 1.01 | -0.01 | 1.02 | 65 | 43 | 47 | 245 | 182 | 26 | | |
| AG 17 | 195007 | 648211 | 2.63 | 1.01 | 1.00 | -0.23 | 1.01 | 320 | 56 | 34 | 140 | 129 | 33 | | |
| AG 18 | 194860 | 648271 | 2.95 | 1.02 | 1.01 | -0.57 | 1.02 | 37 | 10 | 80 | 217 | 278 | 70 | | |
| AG 20 | 194782 | 648841 | 5.04 | 1.01 | 1.01 | 0.05 | 1.02 | 101 | 27 | 63 | 281 | 7 | 9 | | |
| AG 21 | 194777 | 648949 | 3.35 | 1.02 | 1.01 | -0.02 | 1.03 | 34 | 20 | 70 | 214 | 129 | 12 | | |
| AG 23 | 193219 | 646021 | 0.35 | 1.00 | 1.00 | -0.20 | 1.01 | 274 | 3 | 88 | 94 | 5 | 6 | | |
| AG 24 | 193116 | 646192 | 0.46 | 1.03 | 1.01 | -0.49 | 1.04 | 297 | 22 | 68 | 117 | 161 | 61 | | |
| AG 26 | 192825 | 646624 | 3.01 | 1.00 | 1.01 | 0.83 | 1.02 | 87 | 77 | 13 | 267 | 352 | 1 | | |
| AG 34 | 189745 | 645804 | 2.66 | 1.01 | 1.00 | -0.43 | 1.01 | 335 | 20 | 70 | 155 | 241 | 9 | | |
| AB 1 | 200152 | 644446 | 19.80 | 1.02 | 1.01 | -0.33 | 1.04 | 256 | 24 | 66 | 76 | 151 | 31 | | |
| AB 2 | 200182 | 644135 | 5.02 | 1.01 | 1.01 | 0.18 | 1.02 | 251 | 23 | 67 | 71 | 153 | 17 | | |
| AB 3 | 200002 | 643502 | 4.20 | 1.01 | 1.02 | 0.37 | 1.02 | 244 | 35 | 55 | 64 | 124 | 48 | | |
| AB 5 | 200101 | 643219 | 2.71 | 1.01 | 1.02 | 0.37 | 1.02 | 254 | 59 | 31 | 74 | 108 | 26 | | |
| AB 14 | 199153 | 642002 | 2.52 | 1.01 | 1.11 | -0.14 | 1.03 | 283 | 23 | 67 | 103 | 16 | 7 | | |
| AB 15 | 199150 | 641750 | 0.72 | 1.00 | 1.00 | 0.07 | 1.01 | 265 | 16 | 74 | 85 | 53 | 71 | | |

(continued)

Table 1 (continued)

| Sample | 1,000 km grid system | | | | Pole to foliation (K_3) | | | Foliation plane | | | Lineation (K_1) | | |
|--------|----------------------|----------|--------------------------|------|-----------------------------|-------|------|-----------------|--------|-----|---------------------|--------|---------|
| | Easting | Northing | K_{mean} ($E^c - 3$) | L | F | T | P' | Azimuth | Plunge | Dip | Dip azimuth | Plunge | Azimuth |
| AB 17 | 199262 | 641492 | 4.61 | 1.00 | 1.03 | 0.89 | 1.03 | 298 | 36 | 54 | 118 | 199 | 13 |
| AB 19 | 200388 | 641352 | 3.75 | 1.00 | 1.01 | 0.53 | 1.02 | 287 | 31 | 59 | 107 | 18 | 31 |
| AB 21 | 200844 | 641725 | 3.12 | 1.01 | 1.03 | 0.60 | 1.04 | 285 | 36 | 55 | 105 | 127 | 36 |
| AB 23 | 197750 | 644400 | 9.00 | 1.01 | 1.01 | 0.40 | 1.02 | 272 | 53 | 37 | 92 | 139 | 27 |
| AB 26 | 199100 | 645855 | 3.14 | 1.01 | 1.01 | -0.07 | 1.01 | 250 | 5 | 85 | 70 | 3 | 78 |
| AB 27 | 198003 | 641919 | 3.16 | 1.01 | 1.00 | -0.78 | 1.02 | 279 | 21 | 69 | 99 | 183 | 171 |
| AB 28 | 198059 | 641760 | 4.50 | 1.01 | 1.00 | -0.82 | 1.01 | 45 | 34 | 56 | 225 | 169 | 5 |
| AB 29 | 198001 | 641615 | 3.40 | 1.01 | 1.00 | -0.29 | 1.01 | 31 | 56 | 34 | 211 | 191 | 33 |
| AB 32 | 198226 | 639032 | 4.08 | 1.00 | 1.04 | 0.84 | 1.05 | 283 | 38 | 52 | 103 | 116 | 52 |
| AB 33 | 198240 | 638856 | 2.42 | 1.00 | 1.01 | 0.53 | 1.02 | 287 | 37 | 53 | 107 | 156 | 41 |
| AB 39 | 198009 | 646710 | 1.35 | 1.01 | 1.03 | 0.67 | 1.04 | 248 | 66 | 24 | 68 | 123 | 14 |
| AB 42 | 198395 | 643638 | 2.91 | 1.01 | 1.01 | -0.43 | 1.02 | 288 | 30 | 60 | 108 | 188 | 18 |

Fig. 4 AMS parameters for the Northern Arran Granite plotted to show the variation of data and test any potential relationships. **A** P' versus $\text{Log } K_{\text{mean}}$ shows essentially no trend but shows the dominant susceptibility value of 3×10^{-3} . **B** T versus P' shows a very weak positive trend meaning that at higher anisotropies the anisotropy tends toward oblateness

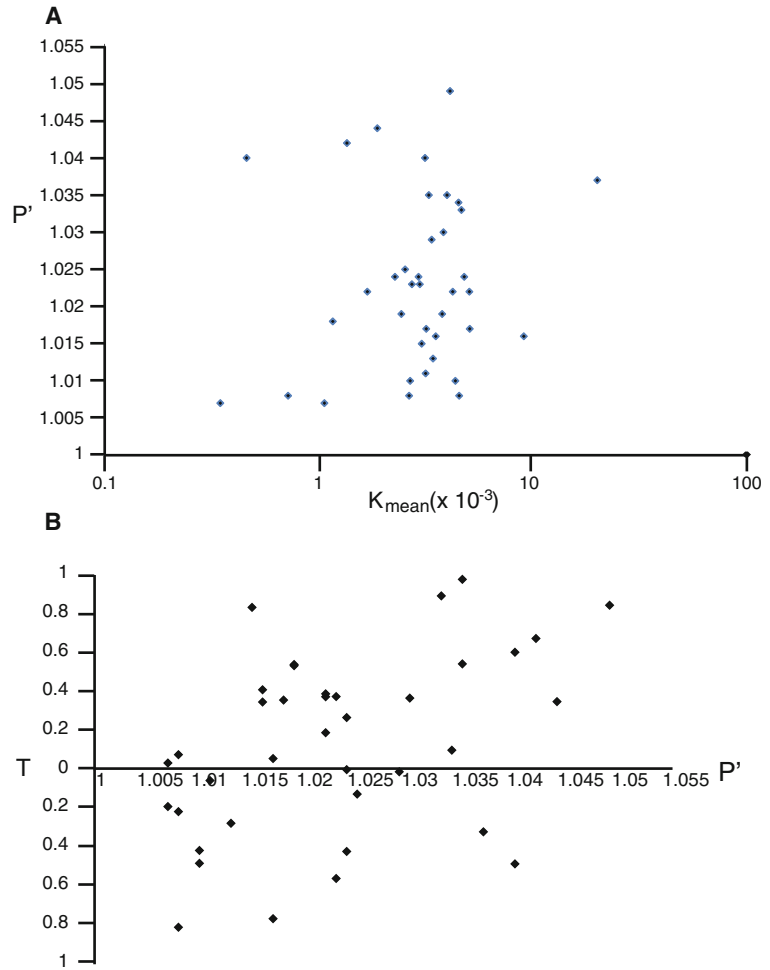


Table 2 Susceptibility values from Palaeogene granitoids from the UK and Ireland

| Intrusion | Susceptibility | Reference |
|---|---|------------------------------|
| Eastern Mourne Granite, NE Ireland | 4.7×10^{-5} – 1×10^{-2} | Stevenson et al. (2007b) |
| Western Mourne Granite, NE Ireland | 1.7×10^{-4} – 5.2×10^{-2} | Stevenson and Bennett (2011) |
| Slieve Gullion porphyritic microgranite, NE Ireland | ca. 1×10^{-2} | Stevenson et al. (2008) |
| Western Red Hills Granite, Skye | Usually $>5 \times 10^{-3}$ (within the range 10^{-4} – 10^{-2}) | Geoffroy et al. (1997) |
| Western Granite, Rum | 2.9×10^{-2} | Petronis et al. (2009) |

crystallised magma was able to concentrate shear close to the internal Inner–Outer Granite boundary. It is also possible that this kind of feature

could identify the boundary between internal granite lobes (sensu Stevenson et al. 2007a; Magee et al. 2012b).

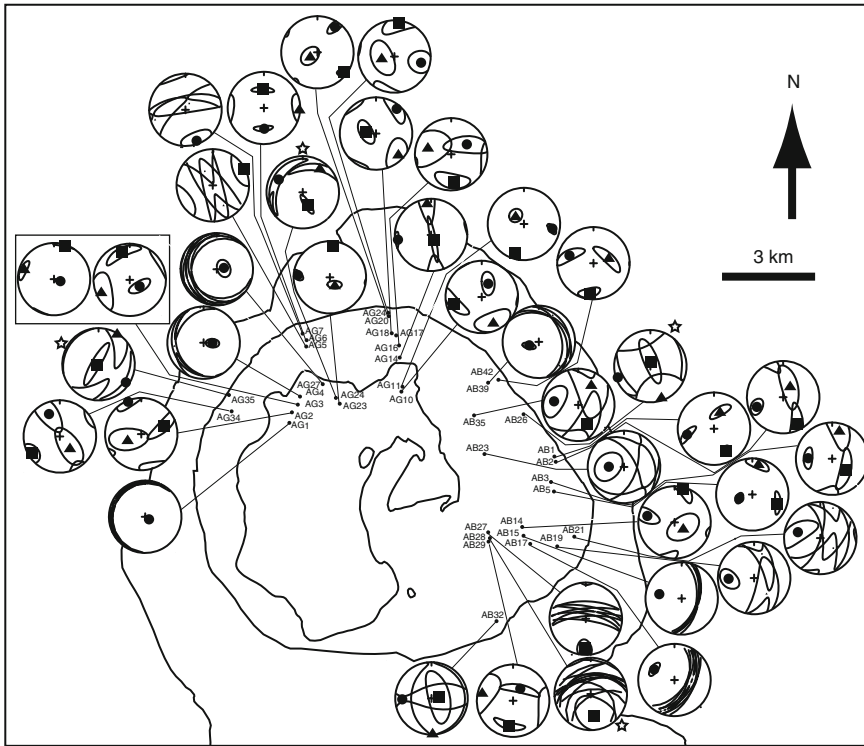


Fig. 5 AMS data plotted stereographically showing the orientation of the principal susceptibility axes for each station. The data for each station has been processed using Jelinek (1981) statistics where the mean orientation is taken using a normalised susceptibility. Confidence ellipses around each axis are 95 % limits. Where no

confidence ellipse is visible the ellipse is smaller than the symbol. Axis symbols: $K_1 = \text{square}$, $K_2 = \text{triangle}$, $K_3 = \text{circle}$. Data where fabrics are weak or the Jelinek statistics do not provide a robust signal are indicated with a *star*

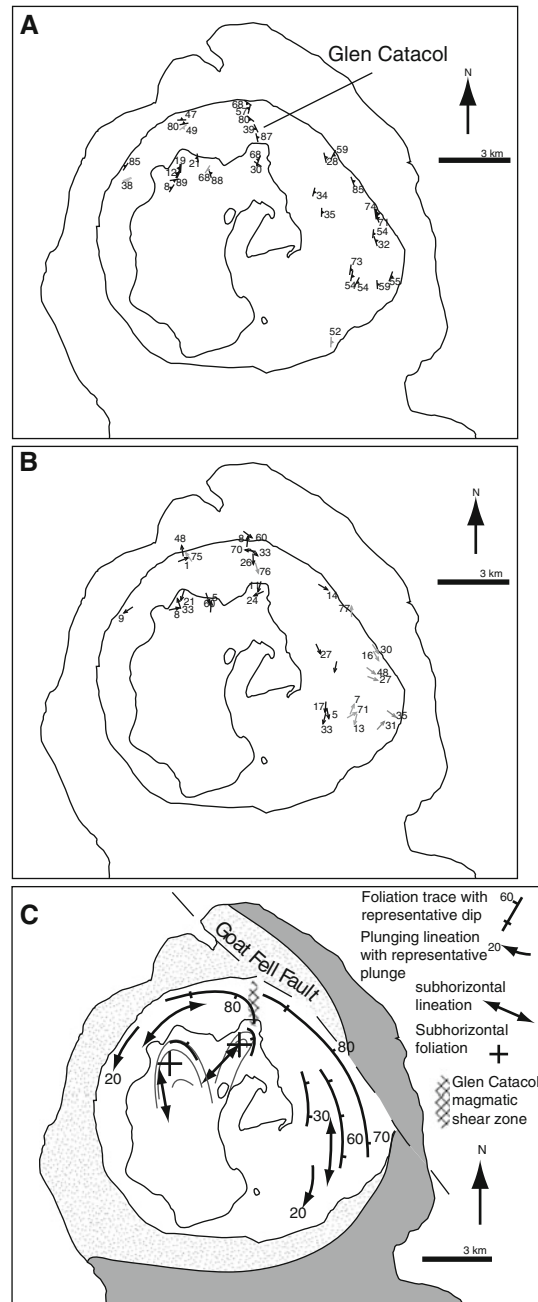
Gouly et al. (2001) gravity modelling suggested that the floor of the pluton lay at 0.3–1.2 km depth. In detail this model indicated a shallower floor in the northwest and the deepest granite in the south east. Although Gouly et al. (2001) concluded that this could be part of England's (1988) diapir model, this depth estimate is at least half the suggested depth in England's (1988) diapir model.

The geometry of the AMS fabrics provides information that enables us to reconstruct the unroofed part of the granite and combine this with the Gouly et al. (2001) gravity model. In the southeast and east, AMS fabrics are concentric and define a partial dome. If we assume the concentric pattern reflects a concordant fabric, we can project the granite contact parallel to the dome shape. This results in a roof that at its

apex would today be projected to roughly 4 km above sea level.

In contrast, the western portions of the pluton contain variable fabrics. Some of these lie within the Inner Granite where the consistent pattern is of gently dipping foliations that parallel mapped contacts (Fig. 6A). Lineations in the Inner Granite are also gently plunging and trend north–south, diverging to the north (Fig. 6B). The Outer Granite fabrics in the north western region do not seem to be concordant with the Inner Granite contacts and we suspect these may preserve parts of or partial lobes or fingers (e.g. Pollard et al. 1975; Stevenson et al. 2007a; Schofield et al. 2010). The Inner Granite seems to form a series of at least two sheets or tongue-like lobes that may coalesce northward and dip south (Fig. 6C).

Fig. 6 Summary of the fabric determined by AMS data. **A** Foliation data plotted using a *strike and dip bar* with a tick indicating dip and dip value stated. Foliations from dominantly linear stations should be viewed with caution and are drawn as *grey symbols*. **B** lineation data plotted using an *arrow* to indicate plunge azimuth and plunge value stated. Lineations from dominantly planar stations should be viewed with caution and are drawn as *grey symbols*. **C** Summary of the AMS fabric data



8.1 Re-examination of Host Rock Deformation

Previous studies have noted the dichotomy of deformation into folding and faulting around the Northern Arran Granite in the Dalradian and post

Caledonian sediments respectively. Folding is dominated by the Catacol Synform affecting only the Dalradian sediments. Doming, in addition, affects post Caledonian sediments, but faulting is the dominant mode of deformation in these younger sediments. This evidence is described in

detail by England (1988, 1992) and Woodcock and Underhill (1987) respectively.

8.1.1 Evidence for Doming of Pre-existing Folds

Sediments above the post Caledonian unconformity display outward dips but are not arranged in a simple dome. Examination of dips along the north eastern shore (from Corrie to Lochranza) indicates a northeast plunging fold that is tighter than the curvature of the granite contact. Woodcock and Underhill (1987) performed an analysis of this fold, the North Sannox anticline, and concluded that it was a conical fold plunging outward consistent with granite related doming. There may be some discordance due to the Goat Fell fault system (Woodcock and Underhill 1987), but we suggest that this conical fold is due to doming, reactivation and modification of a more cylindrical pre-existing east–west trending anticline. We also propose that the variable dip, although mainly outward, in the Devonian sediments directly south of the pluton may also be explained by doming of already folded sediments.

8.1.2 Catacol Synform as the Outer Limit of Laccolithic Doming

The geometry of the Catacol synform was analysed by England (1988, 1992) based on the only onshore exposure of its southeast dipping limb near Newtown (Fig. 2B). We note here however that the strike of this outer limb of this rim synform is not demonstrably deflected around the pluton as would be expected from an expanding diapir model. The strike of the outer limb may be traced in a roughly straight line from the northeast to the southwest with an apparent jog that can be explained by down throw to the northeast across the Goat Fell fault (Fig. 7A, B). Therefore the Catacol synform may simply delineate the extent of upward doming much like examples in the Henry Mountains, Utah, N. America (Johnson and Pollard 1973; Jackson and Pollard 1990;

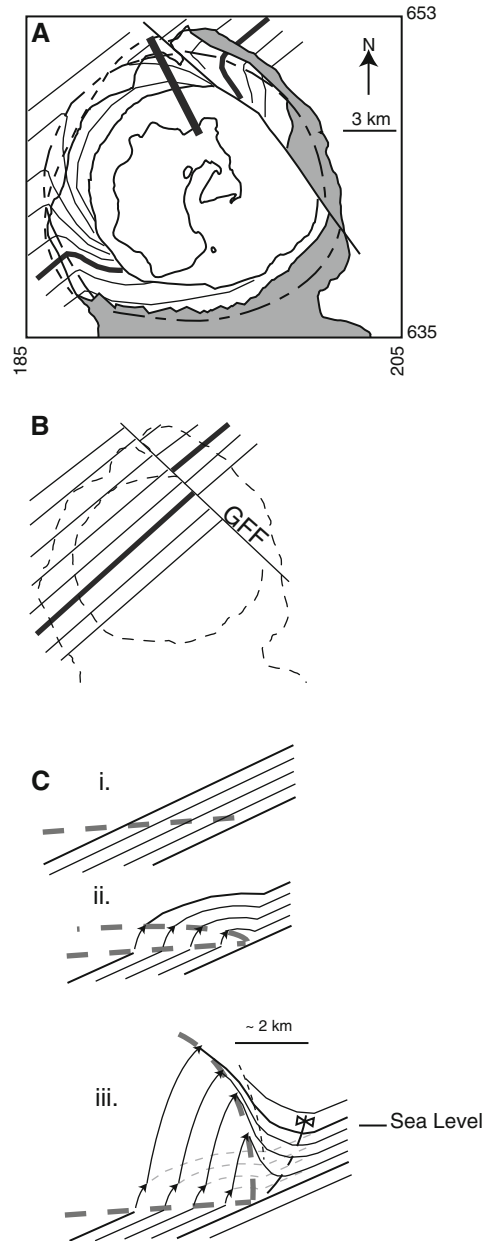


Fig. 7 A Sketch map showing the *strike* of the Dalradian strata highlighting the trace of the Catacol Synform and the Caledonian unconformity. **B** Shows the *strike* of the Dalradian strata without the Catacol synform or the granite. Note the offset across the Goat Fell Fault (GFF). **C** Evolution of the Catacol synform due to doming associated with a laccolith emplacement model for the granite

Horsman et al. 2005), i.e. around a laccolith. In Fig. 7C we outline the development of a concentric rim synform due solely to shouldering from a domed laccolith. Our schematic model uses an approximate scale based on England's (1992) sections. This model allows the Dalradian structure (the Aberfoyle synform) to be reconstructed to pre-granite geometry without a requirement to uplift a large area from beneath 3 km. We have assumed that flexural slip is dominant during the early stages of emplacement of the initial thin sheet, then similar folding takes over where hotter host rocks close to the pluton (in the hornfels zone) and closer to the tip zone of the initial sill flow or deform more. Although our model seems to predict a slightly deeper granite floor than the Goulty et al.'s (2001) gravity model, it demonstrates how a roughly equivalent fold may be generated without a diapir. The evolution and location of the trace of this synform relative to the granite margin depends on dynamic rheology of the aureole.

8.1.3 Reactivation of Pre-existing Transtensional Faults

Woodcock and Underhill (1987) carried out a detailed analysis of brittle deformation around the Northern Arran Granite. These authors noted that the main faulting along the eastern side of the pluton (i.e. the Goat Fell Fault and North Sannox Fault systems) may have initiated before granite emplacement. Here we suggest that, coupled with perpendicular folding (e.g. the Sannox anticline, Fig. 2B) this faulting may represent transtensional faulting caused due to Variscan or early Cenozoic reactivation along the Highland Boundary Fault zone. These faults may have facilitated granite emplacement in a similar way to a bysmalith or 'trap door laccolith' (e.g. Corry 1988; Stevenson et al. 2007b).

The fabric pattern from Glen Catatol (Fig. 6C), if this was fault related, could be a splay off the Goat Fell Fault as it reactivated. This would be

supported if fault related fluid movement was seen to affect the granite in this zone. However this was not examined in this study.

9 Discussion

Our model presents an alternative to the diapir model that fits previously published evidence and is supported by new data. A key tenet of our model is that the Northern Arran Granite must have been emplaced at shallow depths as the adjacent Arran Central Complex (also Palaeogene) contains volcanic lithologies (King 1954). Although the age of emplacement of the latter has not been radiometrically dated, there is evidence that it is younger than the Northern Arran Granite as it cuts southward dipping Devonian strata (domed due to emplacement of the Northern Arran Granite) in the southern aureole of the Northern Arran Granite. Given that the total thickness of the Northern Arran Granite is 4–5 km, and that in the Central Complex there is evidence of Mesozoic cover and probably c. 1 km of denudation, there is a requirement to erode 3–4 km between the emplacement of the Northern Arran Granite and the Arran Central Complex. This may be facilitated by doming associated with the Northern Arran Granite, which was identified by Woodcock and Underhill (1987) as far-field deformation (up to 15 km radius) due to the emplacement of the Northern Arran Granite.

We have suggested that the Northern Arran Granite was emplaced south to north based partly on the south dipping floor (assuming that it was emplaced up dip) but mainly from the north–south trending lineation and the northward divergence in the Inner Granite. This presents the possibility of linking the Northern Arran Granite to the location of a regional gravity high (Emeleus and Bell 2005, p 96). Although a gravity high is more likely to be caused by a mafic complex at depth, the association of felsic and mafic magma in the British and Irish Palaeogene is well

documented (McQuillin and Tuson 1963; Bott and Tuscon 1973; Emeleus and Bell 2005; Gamble 1979) and presents a similar situation to the Mourne Granites and a subjacent laterally offset gravity high (Stevenson and Bennett 2011).

The reason for a northward emplacement may have been due to a thinner post Caledonian overburden north of the Highland Boundary fault zone. This may have allowed the proto-Northern Arran Granite sill to propagate northward dipping gently south, and partly exploiting a pre-existing fold, begin to dome and then form a cupola in the post Caledonian unconformity.

It has been suggested that the Highland Boundary Fault may have provided an ascent route for the Northern Arran Granite magma (e.g. Woodcock and Underhill 1987). However it is also recognised that the HBF is not distinct on Arran, whereas it forms a clear terrane boundary on mainland Scotland (Young and Caldwell 2012). On Arran, the deflection of the basal Devonian unconformity and the Highland Border Complex are the nearest equivalent outcrop expression of this boundary. The HBF's location to the south west onshore Northern Ireland is also ambiguous and is only identified from a geophysical anomaly in a line from Fair Head to Clew Bay, viz. the Fair Head-Clew Bay line. This roughly correlates with the trace of the HBF in Scotland (Max and Riddihough 1975), and stratigraphic correlations made in the West of Ireland (Chew 2003). Most terrane maps show the HBF to be offset left laterally between Northern Ireland and Scotland bending around the Mull of Kintyre (e.g. Woodcock and Strachan 2012, p 33). We suggest here that the HBF may have a significant jog or overstep beneath Arran that provides a focus for magma ascent. The centre of this feature would lie close to the centre of the Island and coincident with the location of the Arran Central Complex and a significant gravity high. This inference presents the possibility of a long lived major crustal structure that could have provided a deeply penetrating ascent route for all the igneous rocks on Arran. Following this the location of the upper crustal magma chamber that fed this activity may have also been controlled by this structure and thus

would have been located beneath the Central Complex and be responsible for the positive gravity anomaly. Sinistral reactivation of the HBF at least pre intrusion of the Northern Arran Granite would explain some weak east-west trending folding and NNW-SSE trending extensional faulting.

9.1 An Emplacement Model for the Northern Arran Granite and the Evolution of the Highland Boundary Fault Zone off Shore Scotland

The pre-Palaeogene structure of the area around Arran was dominated by north-south trending faults, such as the Brodick Bay Fault, that controlled Carboniferous basins in this area (Fig. 1B). It is noteworthy that this activity formed the famous Hutton Unconformity at Catacol Point. The north-south trending faults were probably activated during reactivation of the NE-SW trending HBF during the Variscan Orogeny and acted as a transfer zone between left lateral overstep in the HBF zone that exists in this region. Few obvious NE-SW trending faults exist at the present surface, but it is likely that the HBF zone existed at depth.

During Palaeogene north Atlantic rifting, the HBF was reactivated in a left lateral transtensional sense so the north-south faults offshore Ayrshire and Kintyre acted once again as a transtensional transfer zone (Fig. 8A). This transfer zone likely concentrated magmatism and provided a crustal weak zone facilitating deeply penetrating ascent routes. It is unlikely therefore that magma crossed back and forth across this zone (*sensu* Meade et al. 2009) but probably accessed crustal elements from both sides during its ascent. This ascent site is possibly marked by the major positive gravity anomaly situated beneath the Central Complex.

During Palaeogene rifting, east-west extension focused in a left lateral transtensional transfer zone also generated east-west trending folds exemplified by the North Sannox fold (Woodcock and Underhill 1998). This folding modified the

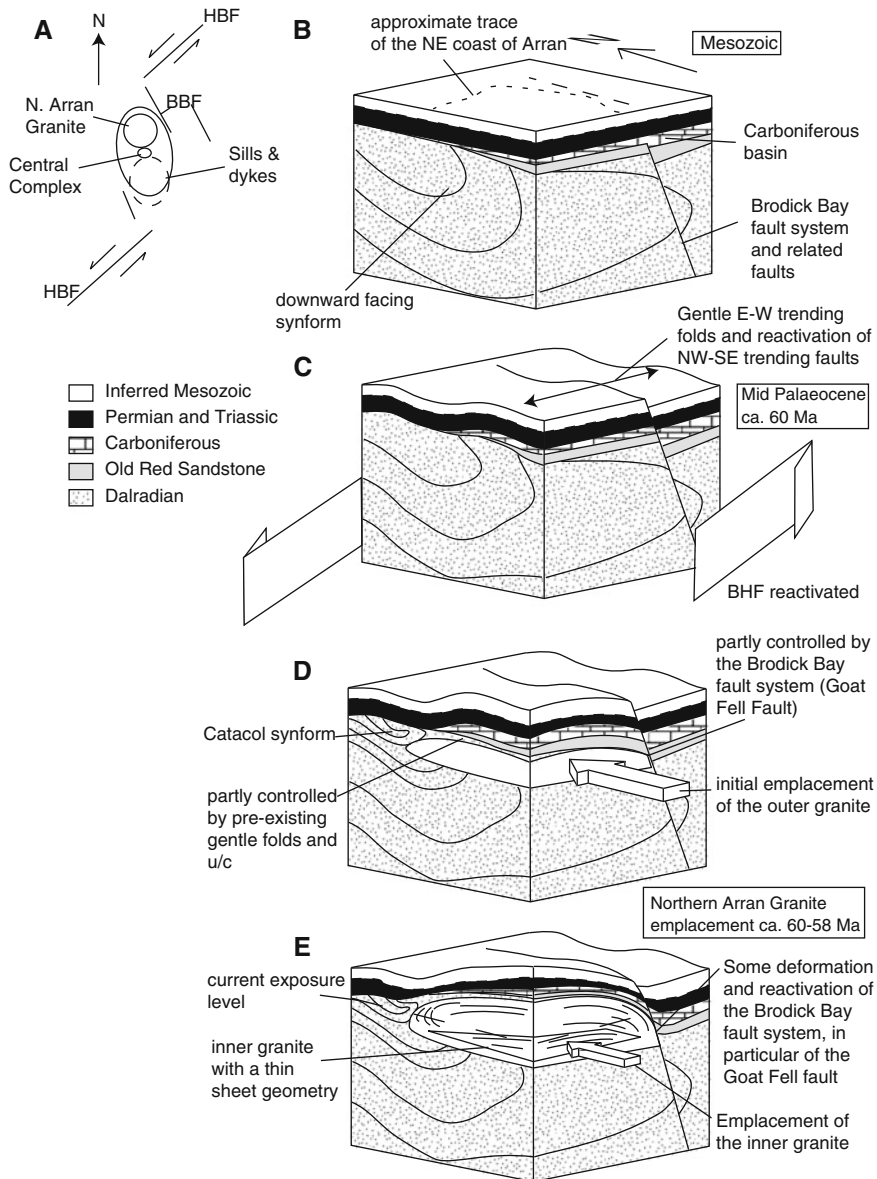


Fig. 8 Final model for the emplacement of the Northern Arran Granite. **A** Schematic representation of the key tectonic elements surrounding Arran highlighting the potential left lateral step in the HBF. **B** Initial stratigraphy pre-Palaeogene. **C** Pre-granite sinistral transension

associated with reactivation of the HBF and focused on the step in the HBF. **D** Initial emplacement of the outer granite from the south as a relatively thin or tabular sheet. **E** Final emplacement stage showing the doming and internal fabric pattern as revealed by AMS data

preexisting downward facing Caledonian folds and created a gently dipping ‘flat’ in the base Permian unconformity next to the HBF (Fig. 8B, C). The timing of this extension relative to the timing of emplacement suggests that extension

began during phase 1 of the NAIP activity (Fig. 3). This extension was at least incipient and may have been focused or concentrated close to pre-existing tectonic structures such as the HBF (cf. Stevenson and Bennett 2011).

The base Permian unconformity NW of the HBF and west of the Brodick Bay fault then acted as a lateral weakness that controlled the emplacement location of the North Arran Granite aided by the flat zone created by the transtensional folding (Fig. 8D). The Inner Granite was emplaced as a gently dipping sheet facilitated partly by further reactivation of the Brodick Bay fault system (Fig. 8D, E).

Thus the Northern Arran Granite was emplaced south to north as an initially thin gently south dipping sheet. As the initial sill thickened vertically, to the east this was accommodated by reactivation of extant north–south trending faults, e.g. the Goat Fell Fault, and by folding and shouldering to the north, west and south—the Catacol Synform.

10 Conclusion

AMS data reveals a subtle internal fabric within the Northern Arran Granite providing information about its emplacement. This fabric describes a gently south dipping laccolith. Steep concordant AMS foliations in the east are consistent with a forceful emplacement and gently dipping foliations in the inner granite suggest that this was emplaced as a gently dipping sheet. Close to the north and north western margins, the foliation pattern can fit with the northward termination of tongue like lobes. The linear component is weak and gently plunging, inconsistent with the diapir model, which warranted a re-examination of the deformed aureole. We demonstrate that the Catacol Synform can be explained by doming and shouldering from a laccolith and does not require several kilometres of uplift. The laccolith was probably emplaced into gentle east-west trending folds created during Palaeogene sinistral reactivation of the HBF zone. The northward emplacement of the granite may have emanated from a deeply penetrating feeder located approximately beneath where the Central Complex is currently situated and there is thus the possibility of a single deeply penetrating crustal ascent route for all the magmatism on Arran, potentially controlled by a left lateral overstep on the HBF zone.

Acknowledgments This work was completed as part of C. Grove's MSci research at the University of Birmingham. We are grateful to M. Binks for field assistance and the Lochranza Distillery for bringing out their first 10 year malt during our field season on Arran.

References

- Anderson EM (1937) The Dynamics of the formation of cone-sheets, ring-dykes and caldron-subsidences. In: *Proceedings of the Royal Society of Edinburgh*, 56:128–157
- Anderson JGC (1947) The geology of the Highland Border: Stonehaven to Arran. *Trans Royal Soc Edinb: Earth Sci* 61:479–515
- Bailey EB (1924) Tertiary and post-tertiary geology of mull, loch aline, and oban: a description of parts of sheets 43, 44, 51, and 52 of the geological map. HM Stationery Office
- Bateman R (1985) Aureole deformation by flattening around a diapir during in situ ballooning: the Cannibal Creek granite. *J Geol* 293–310
- Bell B, Williamson I (2002) Tertiary igneous activity. *Geol Scotland* 371–407
- Borradaile G, Jackson M (2004) Anisotropy of magnetic susceptibility (AMS): magnetic petrofabrics of deformed rocks. In: Martin-Hernandez F, Luneburg CM, Aubourg C, Jackson M (eds) *Magnetic fabric: methods and applications*, geological society, London. Special Publications, London, pp 299–360
- Borradaile GJ, Henry B (1997) Tectonic applications of magnetic susceptibility and its anisotropy. *Earth Sci Rev* 42:49–93
- Bott MHP, Tuson J (1973) Deep structure beneath the Tertiary volcanic regions of Skye, Mull and Ardnamurchan, north-west Scotland. *Nat Phys Sci* 242:114–116
- Bouchez JL (1997) Granite is never isotropic: an introduction to AMS studies of granitic rocks. In: Bouchez JL, Hutton DHW, Stephens WE (eds) *Granite: from segregation of melt to emplacement fabrics*. Kluwer Academic Publishers, Dordrecht, pp 95–112
- Brown DJ, Holohan EP, Bell BR (2009) Sedimentary and volcano-tectonic processes in the British Paleocene Igneous Province: a review. *Geol Mag* 146(03):326–352
- Brun JP, Gapais D, Cogne JP, Ledru P, Vignerresse JL (1990) The Flamanville granite (northwest France): an unequivocal example of a syntectonically expanding pluton. *Geol J* 25(3–4):271–286
- Castro A (1987) On granitoid emplacement and related structures. *Rev Geol Rundschau* 76(1):101–124
- Chew D (2003) Structural and stratigraphic relationships across the continuation of the Highland Boundary Fault in western Ireland. *Geol Mag* 140(01):73–85
- Clemens JD (1998) Observations on the origins and ascent mechanisms of granitic magmas. *J Geol Soc* 155(5):843–851

- Corry CE (1988) Laccoliths: mechanics of emplacement and growth. *Geol Soc Am*
- Cruden AR (1988) Deformation around a rising diapir modeled by creeping flow past a sphere. *Tectonics* 7 (5):1091–1101
- Cruden AR (1990) Flow and fabric development during the diapiric rise of magma. *J Geol* 681–698
- Dickin A, Moorbath S, Welke H (1981) Isotope, trace element and major element geochemistry of Tertiary igneous rocks, Isle of Arran, Scotland. *Trans Royal Soc Edinb: Earth Sci* 72(03):159–170
- Dickin AP (1994) Nd isotope chemistry of Tertiary igneous rocks from Arran, Scotland: implications for magma evolution and crustal structure. *Geol Mag-London* 131:329
- Dickin AP, Bowes DR (1991) Isotopic evidence for the extent of early proterozoic basement in Scotland and northwest Ireland. *Geol Mag* 128(4):385–388
- Doré A, Lundin E, Jensen L, Birkeland Ø, Eliassen P, Fichler C (1999) Principal tectonic events in the evolution of the northwest European Atlantic margin. In: Geological society, London, petroleum geology conference series. Geological Society of London, pp 41–61
- Ellam RM, Stuart FM (2000) The sub-lithospheric source of north atlantic basalts: evidence for, and significance of, a common end-member. *J Petrol* 41(7):919–932
- Emeleus CH, Bell BR (2005) The Palaeogene volcanic districts of Scotland. British Geological Survey
- Emeleus CH, Gyopari M, Britain G (1992) British Tertiary volcanic province. Chapman & Hall, London
- Emeleus CH, Troll VR, Chew DM, Meade FC (2012) Lateral versus vertical emplacement in shallow-level intrusions? The Slieve Gullion Ring-complex revisited. *J Geol Soc* 169(2):157–171
- England RW (1988) The ascent and emplacement of granitic magma: the northern Arran granite. Department of geological sciences, Durham University, Durham, p 212
- England RW (1990) The identification of granitic diapirs. *J Geol Soc* 147(6):931–933
- England RW (1992) The genesis, ascent, and emplacement of the Northern Arran Granite, Scotland: implications for granitic diapirism. *Geol Soc Am Bull* 104 (5):606–614
- Galadi-Enriquez E, Galindo-Zaldívar J, Simancas F, Expósito I (2003) Diapiric emplacement in the upper crust of a granitic body: the La Bazana granite (SW Spain). *Tectonophysics* 361(1–2):83–96
- Gamble JA (1979) Some relationships between coexisting granitic and basaltic magmas and the genesis of hybrid rocks in the Tertiary central complex of slieve-gullion, northeast Ireland. *J Volcanol Geoth Res* 5(3–4):297–316
- Goffroy L, Olivier P, Rochette P (1997) Structure of a hypovolcanic acid complex inferred from magnetic susceptibility anisotropy measurements: the Western Red Hills granites (Skye, Scotland, Thulean Igneous Province). *Bull volcanol* 59(2):147–159
- Gouly NR, Dobson AJ, Jones GD, Al-Kindi SA, Holland JG (2001) Gravity evidence for diapiric ascent of the Northern Arran Granite. *J Geol Soc* 158(5):869–876
- Grout FF (1945) Scale models of structures related to batholiths. *Am J Sci* 243:260–284
- Halliday AN, Graham CM, Aftalion M, Dymoke P (1989) Short paper: the depositional age of the Dalradian Supergroup: U-Pb and Sm-Nd isotopic studies of the Tayvallich Volcanics, Scotland. *J Geol Soc* 146(1):3–6
- Harris A, Baldwin C, Bradbury H, Johnson H, Smith R (1978) Ensialic basin sedimentation: the Dalradian Supergroup. *Crustal Evol Northwest Br Adjacent Reg* 10:115–138
- He B, Xu Y-G, Paterson S (2009) Magmatic diapirism of the Fangshan pluton, southwest of Beijing, China. *J Struct Geol* 31(6):615–626
- Holder MT (1980) An emplacement mechanism for post-tectonic granites and its implications for their geochemical features. In: Origin of granite batholiths. Springer, Berlin, pp 116–128
- Horsman E, Tikoff B, Morgan S (2005) Emplacement-related fabric and multiple sheets in the Maiden Creek sill, Henry Mountains, Utah, USA. *J Struct Geol* 27 (8):1426–1444
- Hutton DHW (1988) Granite emplacement mechanisms and tectonic controls: inferences from deformation studies. *Trans Royal Soc Edinb: Earth Sci* 79(2–3):245–255
- Hutton DHW, Siegesmund S (2001) The Ardara Granite: reinflating the balloon hypothesis. *Zeitschrift der Deutschen Geologischen Gesellschaft* 152(2–4):309–323
- Jackson MD, Pollard DD (1990) Flexure and faulting of sedimentary host rocks during growth of igneous domes, Henry Mountains, Utah. *J Struct Geol* 12 (2):185–206
- Jelinek V (1981) Characterization of the magnetic fabric of rocks. *Tectonophysics* 79(3–4):T63–T67
- Johnson AM, Pollard DD (1973) Mechanics of growth of some laccolithic intrusions in the Henry mountains, Utah, I: field observations, Gilbert's model, physical properties and flow of the magma. *Tectonophysics* 18 (3):261–309
- Jolley DW, Bell BR (2002) The evolution of the North Atlantic Igneous Province and the opening of the NE Atlantic rift. *Geol Soc London Spec Publ* 197(1):1–13
- Jolley DW, Widdowson M (2005) Did Paleogene North Atlantic rift-related eruptions drive early Eocene climate cooling? *Lithos* 79(3–4):355–366
- King BC (1954) The Ard Bheinn area of the central igneous complex of Arran. *Q J Geol Soc* 110(1–4):323–355
- Magee C, Stevenson C, O'Driscoll B, Schofield N, McDermott K (2012a) An alternative emplacement model for the classic Ardnamurchan cone sheet swarm, NW Scotland, involving lateral magma supply via regional dykes. *J Struct Geol* 43:73–91
- Magee C, Stevenson CTE, O'Driscoll B, Petronis MS (2012b) Local and regional controls on the lateral emplacement of the Ben Hiant Dolerite intrusion, Ardnamurchan (NW Scotland). *J Struct Geol* 39:66–82

- Max MD, Riddihough RP (1975) Continuation of the Highland Boundary fault in Ireland. *Geology* 3 (4):206–210
- McLean A, Deegan C (1978) A synthesis of the solid geology of the firth of clyde region. HM Stationery Office
- McQuillin R, Tuson J (1963) Gravity measurements over the Rhum Tertiary Plutonic complex. *Nature* 199 (4900):1276–1277
- Meade FC, Chew DM, Troll VR, Ellam RM, Page LM (2009) Magma Ascent along a major terrane boundary: crustal contamination and Magma mixing at the Drumadoon Intrusive complex, Isle of Arran, Scotland. *J Petrol* 50(12):2345–2374
- Meighan IG, Fallick AE, McCormick AG (1992) Anorogenic granite magma genesis: new isotopic data for the southern sector of the British Tertiary Igneous Province. *Trans Royal Soc Edinb Earth Sci* 83:227–233
- Meyer R, Nicoll GR, Hertogen J, Troll VR, Ellam RM, Emeleus CH (2009) Trace element and isotope constraints on crustal anatexis by upwelling mantle melts in the North Atlantic Igneous Province: an example from the Isle of Rum, NW Scotland. *Geol Mag* 146(03):382–399
- Meyer R, van Wijk J, Gernigon L (2007) The north Atlantic igneous province: a review of models for its formation. *Geo Soc Am Spec Pap* 430:525–552
- Miller RB, Paterson SR (1999) In defense of magmatic diapirs. *J Struct Geol* 21(8–9):1161–1173
- Molyneux SJ, Hutton DHW (2000) Evidence for significant granite space creation by the ballooning mechanism: the example of the Ardara pluton, Ireland. *Geol Soc Am Bull* 112(10):1543–1558
- Mussett AE, Dagley P, Skelhorn RR (1988) Time and duration of activity in the British Tertiary Igneous Province. *Geol Soc London Spec Publ* 39(1):337–348
- O'Driscoll B, Stevenson CT, Troll VR (2008) Mineral lamination development in layered gabbros of the British Palaeogene Igneous Province: a combined anisotropy of magnetic susceptibility, quantitative textural and mineral chemistry study. *J Petrol* 49 (6):1187–1221
- O'Driscoll B, Troll V, Reavy R, Turner P (2006) The Great Euclite intrusion of Ardnamurchan, Scotland: reevaluating the ring-dike concept. *Geology* 34 (3):189–192
- Owens WH (1994) Laboratory drilling of field-orientated block samples. *J Struct Geol* 16(12):1719–1721
- Paterson SR, Fowler TK (1993) Reexamining pluton emplacement processes. *J Struct Geol* 15(2):191–206
- Paterson SR, Vernon RH (1995) Bursting the bubble of ballooning plutons—a return to nested diapirs emplaced by multiple processes. *Geol Soc Am Bull* 107 (11):1356–1380
- Petford N (1996a) Dykes or diapirs? *Earth Environ Sci Trans Royal Soc Edinb* 87(1–2):105–114
- Petford N (1996b) Dykes or diapirs? *Trans Royal Soc Edinb: Earth Sci* 87(1–2):105–114
- Petford N, Clemens JD (2000) Granites are not diapiric! *Geol Today* 16(5):180–184
- Petford N, Cruden AR, McCaffrey KJW, Vigneresse JL (2000) Granite magma formation, transport and emplacement in the Earth's crust. *Nature* 408 (6813):669–673
- Petford N, Kerr RC, Lister JR (1993) Dike transport of granitoid magmas. *Geology* 21(9):845–848
- Petford N, Lister JR, Kerr RC (1994) The ascent of felsic magmas in dykes. *Lithos* 32(1–2):161–168
- Petronis MS, O'Driscoll B, Troll VR, Emeleus CH, Geissman JW (2009) Palaeomagnetic and anisotropy of magnetic susceptibility data bearing on the emplacement of the Western Granite, Isle of Rum, NW Scotland. *Geol Mag* 146(3):419–436
- Pharaoh TC, Morris J, Long CB, Ryan PD (1996) Tectonic map of Britain Ireland and adjacent areas. British Geological Survey, Nottingham
- Pollard DD, Muller OH, Dockstader DR (1975) The form and growth of fingered sheet intrusions. *Geol Soc Am Bull* 86(3):351–363
- Ramberg H (1967) Gravity, deformation and the earth's crust. Academic Press, London
- Ramsay JG (1989) Emplacement kinematics of a granite diapir: the Chindamora batholith, Zimbabwe. *J Struct Geol* 11(1):191–209
- Richey JE (1928) Structural relations of the Mourne Granites (Northern Ireland). *Q J Geol Soc London* 83:653
- Richey JE (1932) Tertiary ring structures in Britian. *Trans Geol Soc Glasgow* 88:776
- Richey JE, Thomas HH (1932) The tertiary ring complex of slieve gullion, Ireland. *Q J Geol Soc London* 88:776–849
- Rubin AM (1993) Dikes verses diapirs in viscoelastic rock. *Earth Planet Sci Lett* 117(3–4):653–670
- Rubin AM (1995) Getting granite dikes out of the source region. *J Geophys Res: Solid Earth* 100(B4):5911–5929
- Sanderson DJ, Meneilly AW (1981) Analysis of three-dimensional strain modified uniform distributions: andalusite fabrics from a granite aureole. *J Struct Geol* 3(2):109–116
- Saunders A, Fitton J, Kerr A, Norry M, Kent R (1997) The north Atlantic igneous province. Large Igneous Provinces: Continental, Oceanic Planetary Flood Volcanism, pp 45–93
- Schmeling H, Cruden AR, Marquart G (1988) Finite deformation in and around a fluid sphere moving through a viscous medium: implications for diapiric ascent. *Tectonophysics* 149(1):17–34
- Schofield N, Stevenson C, Reston T (2010) Magma fingers and host rock fluidization in the emplacement of sills. *Geology* 38(1):63–66
- Shackleton RM (1957) Downward-facing structures of the Highland Border. *Q J Geol Soc* 113(1–4):361–392
- Siegesmund S, Becker JK (2000) Emplacement of the Ardara pluton (Ireland): new constraints from magnetic fabrics, rock fabrics and age dating. *Int J Earth Sci* 89(2):307–327

- Stephenson D, Mendum JR, Fettes DJ, Leslie AG (2013) The Dalradian rocks of Scotland: an introduction. *Proc Geol Assoc* 124(1):3–82
- Stevenson C, Bennett N (2011) The emplacement of the Palaeogene Mourne Granite Centres, Northern Ireland: new results from the Western Mourne Centre. *J Geol Soc* 168(4):831–836
- Stevenson CT, O’Driscoll B, Holohan EP, Couchman R, Reavy RJ, Andrews GD (2008) The structure, fabrics and AMS of the Slieve Gullion ring-complex, Northern Ireland: testing the ring-dyke emplacement model. *Geol Soc London Spec Publi* 302(1):159–184
- Stevenson CTE, Owens WH, Hutton DHW (2007a) Flow lobes in granite: the determination of magma flow direction in the Trawenagh Bay Granite, northwestern Ireland, using anisotropy of magnetic susceptibility. *Geol Soc Am Bull* 119(11–12):1368–1386
- Stevenson CTE, Owens WH, Hutton DHW, Hood DN, Meighan IG (2007b) Laccolithic, as opposed to cauldron subsidence, emplacement of the Eastern Mourne pluton, N. Ireland: evidence from anisotropy of magnetic susceptibility. *J Geol Soc* 164(1):99–110
- Stone P, Kimbell G (1995) Caledonian terrane relationships in Britain: an introduction. *Geol Mag* 132(05):461–464
- Tanner G (2008) Tectonic significance of the highland boundary fault, Scotland. *J Geol Soc* 165(5):915–921
- Tarling D, Hrouda F (1993) *Magnetic anisotropy of rocks*. Springer, Berlin
- Thompson R (1982) Magmatism of the British Tertiary volcanic province. *Scottish J Geol* 18(1):49–107
- Thompson R, Morrison M, Dickin A, Gibson I, Harmon R (1986) Two contrasting styles of interaction between basic magmas and continental crust in the British Tertiary Volcanic Province. *J Geophys Res: Solid Earth* (1978–2012) 91(B6):5985–5997
- Trewin NH (2002) *The geology of Scotland*. Geological Society, London
- Troll VR, Chadwick JP, Ellam RM, Mc Donnell S, Emeleus CH, Meighan IG (2005) Sr and Nd isotope evidence for successive crustal contamination of Slieve Gullion ring-dyke magmas, Co. Armagh, Ireland. *Geol Mag* 142(06):659–668
- Vernon RH, Paterson SR (1993) The ardara pluton, Ireland—deflating all expanded intrusion. *Lithos* 31(1–2):17–32
- Vignerresse JL, Clemens JD (2000) Granitic magma ascent and emplacement: neither diapirism nor neutral buoyancy. *Geol Soc London Spec Publ* 174(1):1–19
- Walker GP (1975) A new concept of the evolution of the British Tertiary intrusive centres. *J Geol Soc* 131(2):121–141
- Wallace J, Ellam R, Meighan I, Lyle P, Rogers N (1994) Sr isotope data for the Tertiary lavas of Northern Ireland: evidence for open system petrogenesis. *J Geol Soc* 151(5):869–877
- Weinberg RF (1996) Ascent mechanism of felsic magmas: news and views. *Earth and Environ Sci Trans Royal Soc Edinb* 87(1–2):95–103
- Woodcock NH, Strachan R (2012) *Geological history of Britain and Ireland*. Wiley, New York
- Woodcock NH, Underhill JR (1987) Emplacement-related fault patterns around the Northern Granite, Arran, Scotland. *Geol Soc Am Bull* 98(5):515–527
- Young GM, Caldwell WGE (2012) The northeast Arran trough, the corrie conundrum and the highland boundary fault in the firth of clyde, SW Scotland. *Geol Mag* 149(4):578–589